

Gamut Mapping in Munsell Constant Hue Sections

Gabriel Marcu

Apple Computer, 1 Infinite Loop, MS: 82-CS, Cupertino, California, 95014

Constant Perceptual Hue in CIELAB

The problem of gamut mapping is of interest in achieving an optimum color reproduction whenever a translation from one device (source) to another device (destination) is requested and the source gamut differs from destination gamut. For printing applications, if the ICC profile specifications are used, gamut mapping is applied to build the color tables that characterize the printing device. Within this approach, the color reproduction performance depends (among other factors) on the ability of the profile to include an efficient mapping method between the device independent color space (referred as the profile connection space, or PCS) and the reproduction device space.

In order to map the out of gamut colors to the colors that can be reproduced on an output device, several mapping methods have been proposed. Most of them use a constant angle section in the CIELAB color space [1-6]. Within this section, different strategies can be used according to the reproduction intent. However the constant angle section in the CIELAB space only approximates the constant perceptual hue. Several studies reported perceptual hue shifts along constant angle section in CIELAB [4-6]. This is why, mapping in constant hue angle in CIELAB space may not give satisfactory performances for certain hue values.

Figure 1 shows in CIELAB space the perceptual hue shift with the variation of lightness [7]. The oblique lines (i.e. segment (1)-(2)) drawn on the exterior of the hue circle illustrate the hue shift in CIELAB for different lightness levels.

The end of the oblique segment closer to the achromatic center of CIELAB section points to the Munsell hue for lightness 2 to 4 (i.e. marked as (1)). The other end of the oblique segment (marked as (2)) points to the same Munsell hue for the lightness 6 to 8. As the segment deviates more from the direction of a hue, the hue shift is larger. For example, the constant hue angle for Munsell 5P hue covers 7 degrees in the CIELAB (a^* , b^*) plane with the variation of Munsell lightness from 4 to 8.

Performing gamut mapping in CIELAB constant angle section can result in perceptual hue error. This error is larger if the mapping procedure modifies the lightness of the mapped color.

To overcome the hue shift, we proposed to perform the gamut mapping in a more uniform space. We pick up for this experiment a space that results from re-mapping the CIELAB coordinate system based on the constraints imposed by the Munsell renotation system. In the Munsell renotation system the colors progress from top to bottom

from very light to very dark in equal intervals. It also offers under daylight viewing conditions, equally perceived light colors for each row and equally perceived chroma on each column.

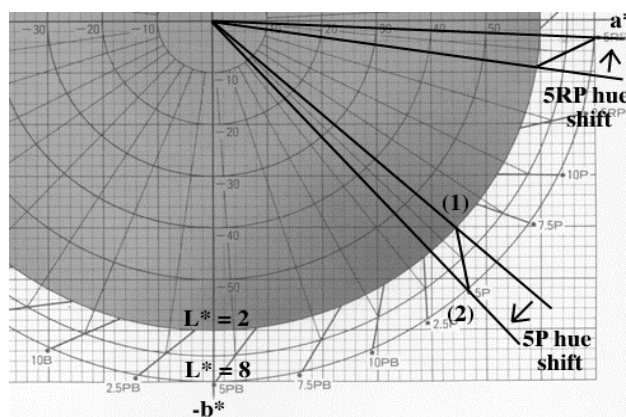


Figure 1. (a^* , b^*) section in CIELAB space illustrating the hue shift for constant Munsell hue.

The new space, referred here as mLAB, uses also $L^*a^*b^*$ coordinates is built such that preserves the lightness of CIELAB but modifies the (a^* , b^*) coordinates of CIELAB system into the (a' , b') coordinates of mLAB such that the constant angle section in the new space fits a constant hue chart of the Munsell renotation system.

The data that is used to perform the conversion is collected from [9] table I (6.6.1). This table defines the (x, y, Y) coordinates of the equally spaced samples in lightness (9 intervals), hue (and chroma. An example of 3D representation in CIELAB coordinates of Munsell samples for 5P and 5RP samples is presented in figure 2.

The samples are collected in the ANSI format file for color data representation. A visualization procedure based on the algorithm introduced in detail by Marcu and Abe in [10] is used to check the data integrity and to illustrate once more the CIELAB hue when varying the lightness. The visualization procedure is not essential and any 3D data visualization package (Mathematica, MathLab, etc) or new emerging languages such as VRML can be used. The transformation from CIE (x, y, Y) to CIELAB used D65 as reference white. The visualization procedure illustrates in 3D the hue shift that is depicted in 2D in figure 1. It can be observed from both representations (figure 1 and 2) that for RP and P the hue shift has opposite directions.

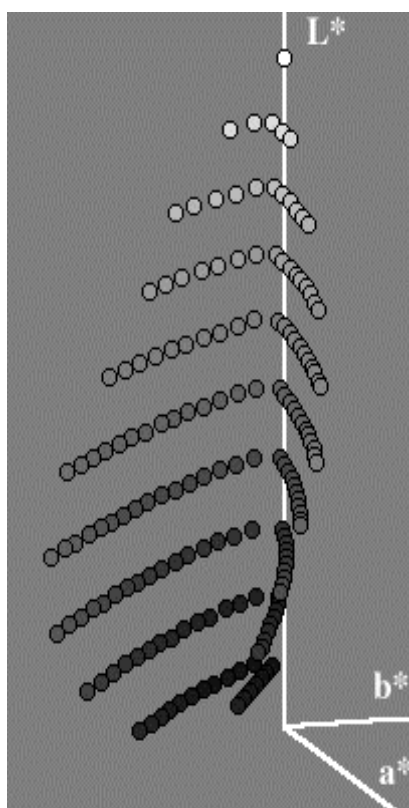


Figure 2. 3D representation of two constant Munsell hue sections (5P and 5RP)

The hue shift can be observed both along chroma variation for each constant value and along the value variation. This diagram illustrates clearly that constant lightness mapping procedures provide better protection against hue shift than the procedures that modify also the lightness. The hue shift is bigger if the mapping procedure modifies the lightness of the mapped color. Even if 5P and 5RP are relatively close, their hue shift is not in the same direction when lightness decreases.

The CIELAB – mLAB Conversion

A color conversion method between the CIELAB and mLAB space is described based on a set of fix points and interpolations. The modified CIELAB space is a perceptual linear CIELAB space and is referred as mLAB.

The transformation procedure is performed using a tetrahedral interpolation algorithm in CIELAB space [11]. The unknown color is interpolated from four known Munsell colors that determine the minimum tetrahedron that includes the unknown color.

The tetrahedrons can be identified in two ways. The first approach uses a searching procedure to find the interpolation tetrahedron. The searching procedure finds the first closed N Munsell values to the unknown color and then checks the inclusion condition for each combination of four colors (from the set of N) determining a tetrahedron. Since the searching procedure can find more than a tetrahedron

that includes the unknown color, an additional criterion can be used to select the best tetrahedron (the tetrahedron that will give the smaller interpolation error). We found that the standard deviation of the face angle values of each tetrahedron from the selected candidates can give a good measure of tetrahedron “compactness”, and this was correlated with the minimum interpolation error. Even without this criterion, the searching procedure can give acceptable results even if the first tetrahedron to verify the inclusion condition is selected for interpolation. For our experiment N was limited to the closest 15 Munsell colors to the unknown color. This leaves a number of 1365 tetrahedrons to be investigated for each unknown color.

A second approach to decompose the CIELAB space in disjoint and adjacent tetrahedrons. This implies to pre-compute all tetrahedrons determined by the Munsell set and then to use an indexed procedure to find the tetrahedron that includes the unknown color. In either case, once the tetrahedron is identified, the interpolation procedure is performed based on the following set of equations:

$$C = a1. C_{m1} + a2. C_{m2} + a3. C_{m3} + a4. C_{m4} \quad (1)$$

$$C' = a1. C'_{m1} + a2. C'_{m2} + a3. C'_{m3} + a4. C'_{m4} \quad (2)$$

where C_{m1} , C_{m2} , C_{m3} , C_{m4} represent the CIELAB vectors of the Munsell set, C'_{m1} , C'_{m2} , C'_{m3} , C'_{m4} represent the vectors in the mLAB space, $a1, a2, a3, a4$ represent the barycentric coordinates of the unknown color in the tetrahedron, and C and C' represent the unknown color and its correspondent in the mLAB. For the reverse conversion the searching procedure is not required due to the regular structure of the mLAB linear space.

The Munsell renotation system does not cover all the CIELAB values required to fill in for 3D color tables of an ICC profile if CIELAB is used as the PCS. To overcome this problem, the CIEXYZ is selected as PCS and only a subset of values of CIEXYZ corresponding to an area covering all practical CRTs and LCDs devices on the market today is selected for computations. However a “gamut” checking is performed to prove that the limited CIEXYZ space is covered by the samples offered by Munsell renotation system. The equation (1) and (2) are used to verify that none of the colors required to build the XYZ to device or device to XYZ tables of the ICC profile are not left out of the tetrahedrons defined within the Munsell renotation system.

As it is implemented, the searching procedure is time consuming. However the procedure is performed off line, to build the ICC profile tables. It does not affect the processing time of the image. This time is determined only by the color transformation engine of the CMS. For a 166Mhz Power PC, the procedure requires less than 5 minutes to run for a table of $17 \times 17 \times 17$ elements.

Gamut Mapping Using the Linear CIELAB Space

The mLAB space is used to perform the gamut mapping. The diagram of the transformations required to fill in the 3D tables of the ICC profile is presented in figure 3.

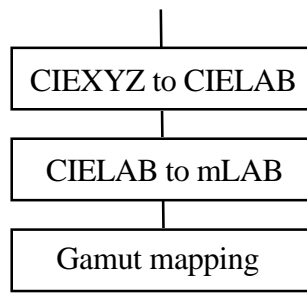


Figure 3. The diagram of the color transformation to support gamut mapping in the linear CIELAB space.

The mapping procedure in the mLAB space can use the same mapping functions as the constant angle mapping in CIELAB space. The difference now is that the L'a'b' values of a color in mLAB space really represent the perceptual constant hue and chroma according to the definition of the Munsell renotation system. Therefore the proposed method combines the advantage of color specification of the CIELAB space with the advantage of the uniform perceptual color specification in the Munsell renotation system.

In order to compare the gamut mapping performed in Munsell constant hue section versus the one performed in CIELAB constant hue angle, the following strategies are investigated:

- (a)-constant lightness;
- (b)-constant saturation;
- (c)-combination of (a) and (b);
- (d)-mapping to a defined center of the gamut;
- (e) mapping to a variable achromatic point;

These procedures are briefly described in the figure 4, 5 and 6. It can be noted that the 2D description of these procedures really represents constant perceptual hue sections in the mLAB space.

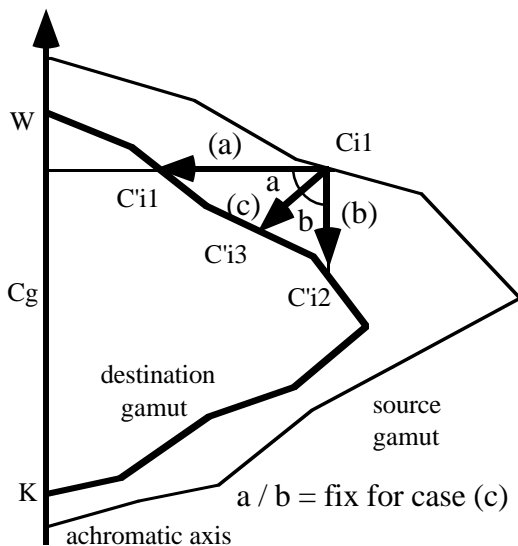


Figure 4. Gamut mapping based on constant lightness (a), constant saturation (b), and on combination of (a) and (b)

In figure 5, the method (d) clips the out of gamut colors on the gamut surface toward the gravity center of the destination gamut. The gravity center, C_g, is selected on the achromatic axis at 50% between the black and white achromatic axis of the destination gamut. Perceptually, this method proved to give more pleasant results than saturation clipping (b) or lightness clipping (a). The method (c) and (d) keep a balance between the error of saturation and lightness.

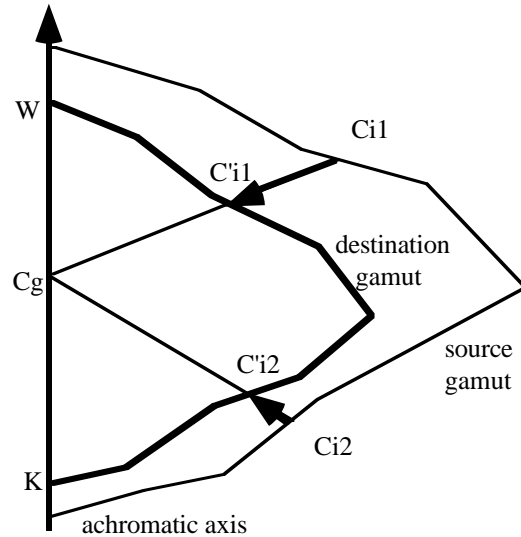


Figure 5. Gamut mapping to the gamut center (method (d))

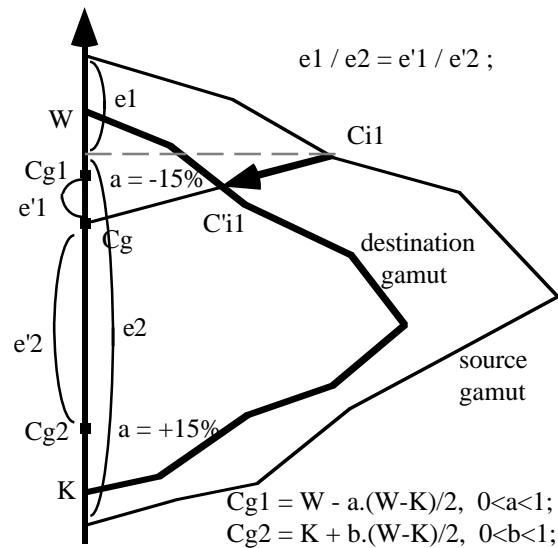


Figure 6. Gamut mapping to a variable achromatic point (method (e)).

In figure 6, the method (e) uses instead of the fix gravity center a variable point (C_g in figure 6) that is dynamically computed and that can migrate between two fix points, C_{g1} and C_{g2}, of the achromatic axis of the destination gamut. The position of the points C_{g1} and C_{g2}

is selected empirically lower than the lighter and higher than the darker points of the destination gamut (15% in our experiment). The position of the center Cg between the fix points Cg1 and Cg2 is determined based on the luminance level of the color to be mapped, Ci1, in the source gamut. This position is determined with respect to the whiter and darker points of the source gamut and is described by the ratio $e1/e2$ on the achromatic axis of the source gamut. The center Cg is selected between Cg1 and Cg2 such that the ratio $e'1 / e'2 = e1 / e2$ as it is illustrated in figure 6.

Results

The comparison of the mapping strategies has been performed by 5 subjects on 6 printed samples. The gamut mapping was used for a profile of the Color Style Writer 6500 printer. The samples are a mixture of SCID data (bitmaps) and graphic data (vectors). The printed samples were viewed in a light booth, under D50 illuminant. The original image was displayed on a calibrated CRT monitor (AppleVision 850 display, 1.8 gamma with D50 white point).

Table 1. Gamut mapping performed in mLAB (A) versus CIELAB (B) constant hue angle for method (e) for 5 observers (1~5).

Image	1	2	3	4	5
Lady	A	A	A	A	A
Market	A	B	A	A	A
Fruits	A	B	A	B	A
Musicians	A	A	A	A	A
Bicycle	B	A	A	A	A

For one comparison, each observer is presented with 3 images: the original on the screen, and 2 printed samples, (A) and (B), produced with the same gamut mapping strategy. The print sample (A) uses mLAB constant angle gamut mapping while the print sample (B) uses CIELAB constant angle gamut mapping. The observer was requested to mark the preferred image. The experiment was repeated for each mapping strategy. Due to limited paper space, only one sample table derived for the procedure (e) is presented in table 1.

Conclusion

This paper presents a color conversion between Munsell notation system and the CIELAB color space.

The conversion was used to improve gamut mapping methods performed in constant hue angle sections in CIELAB.

The color conversion to/from the linear CIELAB (mLAB) does not cover all possible CIELAB colors, but enough colors to fill in the 3D tables required for an ICC profile. Several gamut mapping methods were investigated. The evaluation proves that the Munsell constant hue section is preferred against CIELAB constant hue angle (21 votes against 4). In all cases, the perceptual hue mapping is preferred against the CIELAB constant angle mapping. From all experiments it appears also that the strategy 5 are preferred against 1, 2 and 3. The experiment is still in progress, collecting the observations from a larger number of observers.

References

1. M. Stone and J. Beaty, Color gamut mapping and the printing of digital color images, *ACM Transaction on Graphics*, **V7**, p.249-292 (1988).
2. W. Wallace and M. Stone, *Gamut mapping computer generated imagery, SPIE V1460: Image Handling and reproduction systems integration* p.20-28 (1991).
3. R. S. Gentile, E. Walowitz and J. P. Allebach, A comparison of color gamut mismatch compensation, *J. Imaging Technol.*, **V16**, p.176-181 (1990).
4. M. Wolski, J. P. Allebach and C. A. Bouman, Gamut mapping, squeezing the most out of your color system, 2nd Color Imaging Conference, p.89-92 (1994).
5. P. C. Hung and R. Berns, Determination of constant hue loci for a CRT gamut and their prediction using color appearance spaces, *CR&A*, **V20**, p/285-295 (1995).
6. N. Katoh and M. Ito, Gamut mapping for computer generated images, *4th Color Imaging Conference*, p.126-129 (1996).
7. F. Ebner and M. D. Fairchild, Gamut mapping from bellow: Finding minimum perceptual distances for colors outside the gamut volume, *CR&A V22(6)* p.402-413 (1997).
8. Minolta, Precise color communication-color control from feeling to instrumentation, User's manual, Chroma meter CR-100 Series.
9. G. Wyszecki and W. S. Stiles, *Color Science: Concepts and Methods, Quantitative data and Formulae*, Second edition, John Wiley & Sons, p.507, and p.840~852 (1982).
10. G. Marcu and S. Abe, Three dimensional histogram visualization and applications, *JEL*, **V4 (4)**, p.26-43 (1995).
11. P. C. Hung, Colorimetric calibration in electronic imaging devices using look-up table model and interpolations, *JEL V2(1)* 1993.